SCIENTIFIC Publishing Limited

New Energy Exploitation and Application

http://ojs.ukscip.com/index.php/neea

Article

New Methanation Reactor by Reciprocating Engine (MeRE)

Kazuhiro Yamamoto * **and Yuya Matsuura**

Department of Mechanical Systems Engineering, Nagoya University, Nagoya 464-8603, Aichi, Japan

* Correspondence: kazuhiro@mech.nagoya-u.ac.jp; Tel.: +81-52-789-4471

Received: 26 July 2024; **Revised:** 10 December 2024; **Accepted:** 15 December 2024; **Published:** 16 December 2024

Abstract: Methanation, which synthesizes methane from carbon dioxide and hydrogen, can potentially be an important core technology for realizing a carbon-neutral society. A catalyst is normally used in the methanation process, but its thermal degradation is a serious problem. Thus, we have proposed a catalyst-free methanation reactor that simulates an internal combustion engine. We call it a Methanation Reciprocating Engine (MeRE), where the up-and-down motion of the piston inside the engine creates a high-temperature, high-pressure field inside the reactor that is suitable for the methanation reaction. In this study, we conducted a 0-dimensional simulation using a program package, Chemkin-II. To make clear the reactor characteristics based on the reaction process in the MeRE, we used an ICEN code (Internal Combustion Engine) to simulate the MeRE. We changed the initial temperature, the components of reactants, the rotational speed, and the compression ratio. It is found that the reaction rate of methane production can be enlarged by increasing the initial temperature, the compression ratio, and the rotational speed. Additionally, it is better to set the composition which is close to the stoichiometric ratio of the Sabatier reaction. For all cases, the CO_2 conversion rate is high, but the CH_4 selectivity is very low. Resultantly, in the case of the MeRE, it is easy to produce CO from CO_2, while the reaction which converts from CO to CH_4 is unlikely to take place.

Keywords: Renewable Energy; Methanation; Hydrogen; Synthetic Natural Gas; Internal Combustion Engine

1. Introduction

In recent years, global warming has become more serious. Since the Paris Agreement was adopted at the 21st Conference of the Parties to the United Nations Framework Convention on Climate Change (COP21) in 2015 [1], countries in the world have taken various measures against climate change. The recent COP28 is a part of ongoing efforts to reduce greenhouse gas emissions. Apart from addressing climate change and unsustainable resource extraction, it also addresses how oil and gas companies could influence climate policies [2]. In Japan, we declare to achieve carbon neutrality by 2050 [3]. It is reported that the energy conversion sector including power generation and petroleum refining accounts for 40.4% of carbon dioxide emissions in Japan. In the power generation category, in particular, the amount of CO_2 emission might be enlarged significantly due to the restart of thermal power plants and the construction of new thermal power plants after the Great East Japan Earthquake in 2011. This situation is undesirable from the perspectives of both CO_2 reduction and energy security in Japan, which depend almost entirely on fossil fuels from overseas for primary energy. Therefore, in 2017, our government formulated the basic strategy for hydrogen by treating hydrogen as a new energy option. It is reported that hydrogen is expected to be carbon-free fuel and can be an energy carrier for storing, transporting, and utilizing renewable energy that is susceptible to environmental factors [4].

It is well-noticed that methanation is one of the technologies that have attracted attention as a way to utilize hydrogen. It is used to synthesize methane from carbon dioxide and hydrogen [5–9]. It is considered that the

fuel synthesized by methanation is carbon neutral because hydrogen is produced using surplus electricity from renewable energy sources and carbon dioxide is recovered from power plants and factories [10–12]. Since methane is the main component of natural gas, existing infrastructure facilities such as gas pipelines and gas consumption equipment can be used without any modification [4, 13]. Renewable energies such as solar power and wind power are usually affected by the natural environment in terms of the amount of electricity they generate [14–16]. Methane converts renewable energy into gaseous fuels for storage and utilization, corresponding to a Power-to-Gas (PtG) technology [7, 17].

In conventional methanation reactors, high reaction efficiency is achieved by using catalysts that accelerate the reaction [17]. However, because methanation is an exothermic reaction, the formation of a local high-temperature region (hot spot) causes the thermal deactivation of the catalyst [18]. There may be also the problem of chemical degradation of the active metal due to impurities in the feedstock gas [19]. Although the thermal degradation of the catalyst is avoided by using a cooling system with a heat exchanger, a thermally controlling system is needed, which makes the reactor larger and more complicated, resulting in an increase of the excessive costs. Then, in our previous research, we have proposed a reactor, called MeRCi (Methanation Reactor with Circulation), which can effectively utilize the heat of reaction in methanation and control the catalyst temperature without any heat exchangers [20].

As explained, when no catalysts are used, the thermal degradation of the catalyst does not need to be considered, and costs can be significantly reduced. In the present paper, as another type of reactor, we are developing a catalyst-free methanation reactor that simulates an internal combustion engine. We call it a Methanation Reciprocating Engine (MeRE), which is shown in **Figure 1**. The up-and-down motion of the piston inside the engine creates a high-temperature, high-pressure field inside the cylinder that is suitable for methanation reactions, allowing the engine to be used as a methanation reactor. In this study, we conducted a 0-dimensional simulation using a program package, Chemkin-II [21] developed by the Sandia National Laboratories. It is a software package for facilitating the formation, solution, and interpretation of problems involving elementary gas-phase chemical kinetics. It provides an especially flexible and powerful tool for incorporating complex chemical kinetics into simulations of fluid dynamics. The package consists of two major software components: an Interpreter and Gas-Phase Subroutine Library. The Interpreter is a program that reads a symbolic description of an elementary, user-specified chemical reaction mechanism. One output from the Interpreter is a data file that forms a link to the Gas-Phase Subroutine Library. The main objective was to investigate the effectiveness of the MeRE, but we tried to find optimal operating conditions for the reactor. To realize the conditions of the internal reciprocating engine, the calculations were performed in ICEN code (Internal Combustion Engine). Here, we focused on the four factors deeply related to the reactiveness of the engine operation. They were the initial temperature, the components of reactants, the rotational speed, and the compression ratio, which were apparently independently changed in the operating system.

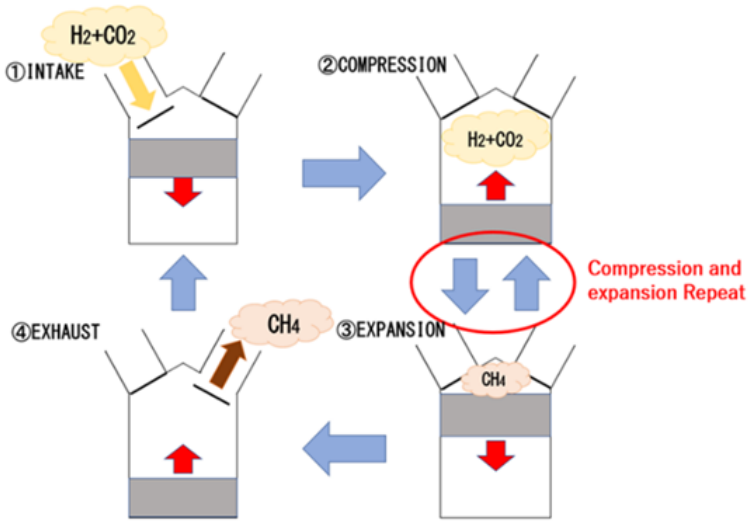

Figure 1. A schematic of methanation reciprocating engine (MeRE).

2. Numerical Model

Here, we explain the methanation reaction [22–27], which is described in Equation (1).

$$CO_2 + 4H_2 = CH_4 + 2H_2O + 165\text{kJ/mol} \tag{1}$$

It is called the Sabatier reaction because Paul Sabatier discovered this reaction. It is seen that the raw materials are carbon dioxide and hydrogen. The Sabatier reaction consists of two reactions, which are shown below.

$$CO_2 + H_2 = CO + H_2O - 41\text{kJ/mol} \tag{2}$$

$$CO + 3H_2 = CH_4 + H_2O + 206\text{kJ/mol} \tag{3}$$

In these equations, the heat of reaction calculated by the standard enthalpy of formation for each species is described. It is noted that the reaction in Equation (2) is called the reverse water-gas shift reaction, and the reaction in Equation (3) corresponds to the CO methanation.

For evaluating the suitable methanation conditions, the CO_2 (or H_2) conversion rate and CH_4 (or CO) selectivity were introduced to discuss the methanation reaction [28]. The CO_2 or H_2 conversion rate shown in Equation (4) is an index that examines how much carbon dioxide or hydrogen in the reactant is converted to other substances.

$$P_{CO_2(H_2)}[\%] = \frac{\frac{Y_{in,CO_2(H_2)}}{44(2)} - \frac{Y_{out,CO_2(H_2)}}{44(2)}}{\frac{Y_{in,CO_2(H_2)}}{44(2)}} \times 100 \tag{4}$$

On the other hand, the CH_4 (or CO) selectivity in Equation (5) shows how much of the carbon dioxide is converted to CH_4 or CO.

$$S_{CH_4(CO)}[\%] = \frac{\frac{Y_{out,CH_4(CO)}}{16(28)}}{\frac{Y_{in,CO_2}}{44} - \frac{Y_{out,CO_2}}{44}} \times 100 \tag{5}$$

In Equations (4) and (5), $Y_{in,i}$ is the initial mass fraction of species i before the reaction starts, and $Y_{out,i}$ is the mass fraction of species i in the outflow gas from the reactor. In Chemkin-II, the input data for chemical species must be given in terms of molar ratios or mole fractions, and the output data are in terms of mole fractions, so the mole fractions are converted to mass fractions to obtain the above CO_2 or H_2 conversion rate and the CH_4 or CO selectivity.

Next, the numerical conditions are described. In this study, we focused on the initial temperature, the components of reactants, the rotational speed, and the compression ratio, which are input parameters in the ICEN code. The initial temperature was varied from 600 K to 800 K. The rotational speed was from 300 to 900 rpm, and the compression ratio was from 10 to 20. The reaction time was 1000 s in each case.

3. Results and Discussion

3.1. Effect of Initial Temperature

First, the effect of the initial temperature was investigated. The results are shown in **Figure 2**. The initial pressure was 1 atm, the initial composition was H_2:CO_2 = 4:1, the compression ratio was 15, and the rotational speed was 600 rpm. As seen in **Figure 2a**, when the initial temperature was 800 K, the CO_2 conversion rate was 96.3%. It is found that the difference between values at the top dead center (TDC) and at the bottom dead center (BDC) at the initial temperature of 800 K becomes larger after 200 s. This could be due to the fact that both the temperature and the pressure at TDC largely increase inside MeRE, resulting in the formation of a large number of radicals which accelerate the conversion from CO_2 to CO.

On the other hand, in the time-variation of the H_2 conversion rate shown in **Figure 2b**, it is found that the higher the initial temperature, the higher the H_2 conversion rate. That is, in comparison with the CO_2 conversion rate, the same trend is observed. However, when the initial temperature was 800 K, the maximum H_2 conversion is only 26.9%, which is much smaller that the CO_2 conversion rate. Resultantly, it is only a quarter of the maximum CO_2 conversion rate.

For further discussion, the time-variation of the CH_4 selectivity is shown in **Figure 2c**. Only in the early stage of the reaction, it is seen that the higher the initial temperature, the larger the CH_4 selectivity. However, at the

highest initial temperature of 800 K, the CH_4 selectivity reaches a maximum roughly at 150 s and then decreases. That is, the CH_4 selectivity is reduced when the temperature inside the reactor is high. Based on our previous chemical equilibrium calculations [19], it is found that methane production increases when the initial temperature is relatively lower. By taking Le Chatelier's principle into account, it is reasonable, because the Sabatier reaction in Equation (1) is exothermic.

For comparison, we checked the CO selectivity. Results are shown in **Figure 2d**. For all initial temperatures, the CO selectivity immediately reaches 99.9%, and then decreases slightly as the reaction proceeds. It can be said that Equation (2) is the main reaction, and the reaction rate of Equation (3) is much smaller. We conclude that the increase of the initial temperature enlarges the reaction rates of the CO_2 and H_2 consumptions, but the higher initial temperature reduces the CH_4 or CO selectivity. There could be an optimum temperature that is suitable for the methanation. In all cases, the CO selectivity is much larger than the CH_4 selectivity, confirming that it is easy to produce CO from CO_2, while the reaction where CO is converted to CH_4 is unlikely to take place.

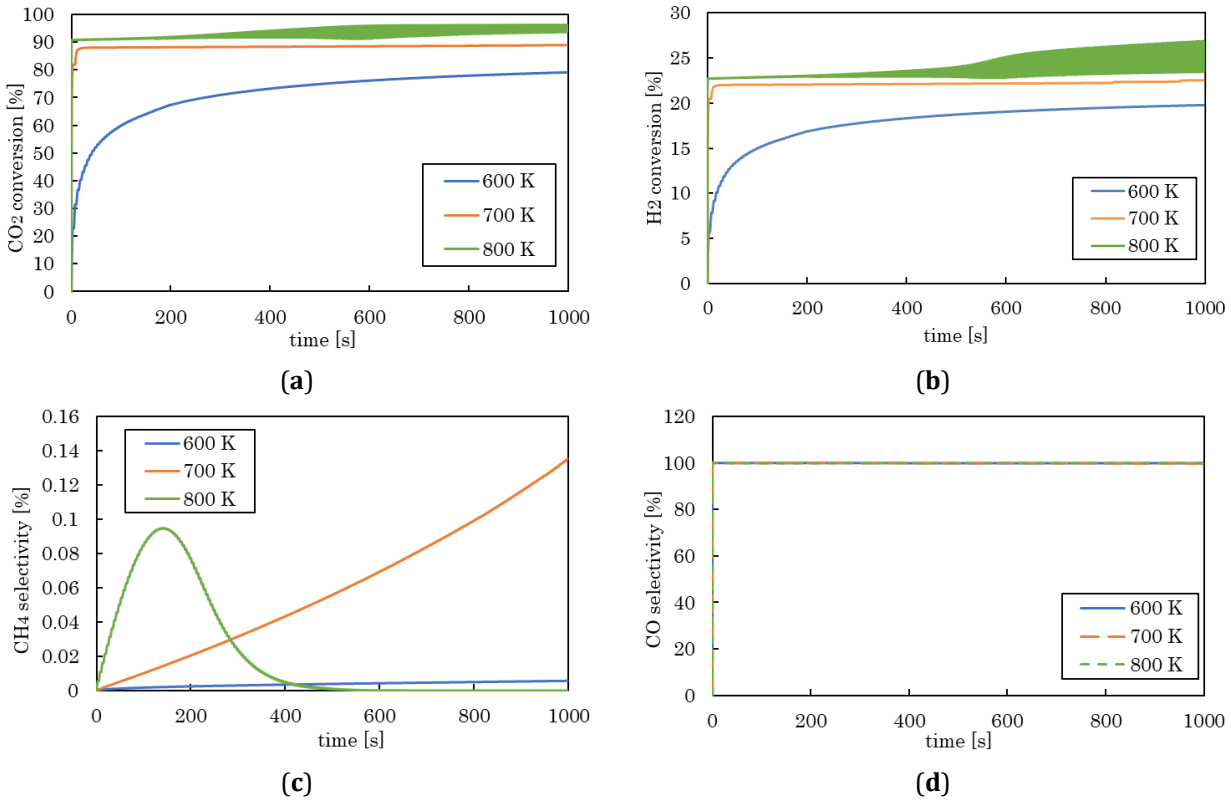

Figure 2. Effects of the initial temperature on the time-variations of (**a**) CO_2 conversion rate; (**b**) H_2 conversion rate; (**c**) CH_4 selectivity; (**d**) CO selectivity.

3.2. Effects of Components of Reactants

Next, we changed the initial components of the reactants, carbon oxide and hydrogen. The results are shown in **Figure 3**. The initial pressure was 1 atm, the initial temperature was 600 K, the compression ratio was 15, and the rotational speed was 600 rpm. As shown in **Figure 3a**, the higher the hydrogen content, the higher the CO_2 conversion rate. This is because the reaction in Equation (2) is accelerated when more hydrogen is supplied. Resultantly, the CO_2 conversion rate increases. When the initial composition is H_2:CO_2 = 10:1, the CO_2 conversion rate is 95.5%.

Figure 3b shows the time-variation of the H_2 conversion rate. Initially, when more hydrogen is supplied, the increasing rate of the H_2 conversion rate is large, but the final value of the H_2 conversion rate is relatively low. This is because the Sabatier reaction in Equation (1) is promoted by increasing the hydrogen concentration in the

reactants, with the higher hydrogen conversion rate, but the excess hydrogen remains unreacted after the reaction. When the initial composition is stoichiometric, the H_2 conversion ratio is only 19.8%.

Figure 3c shows the CH_4 selectivity as a function of time, indicating that the higher the hydrogen content, the larger the CH_4 selectivity. This is because the reaction in Equation (3) is accelerated when more hydrogen is supplied, and the methane production increases. When the initial composition is H_2:CO_2 = 10:1, the CH_4 selectivity is 0.324%, which is unexpectedly low. Thus, it is derived that the higher the hydrogen content, the higher the CO_2 conversion and the CH_4 selectivity. However, the final values of the H_2 conversion and the CH_4 selectivity are lower even at higher hydrogen concentration in the reactants because of the large deviation from the stoichiometry of the Sabatier reaction.

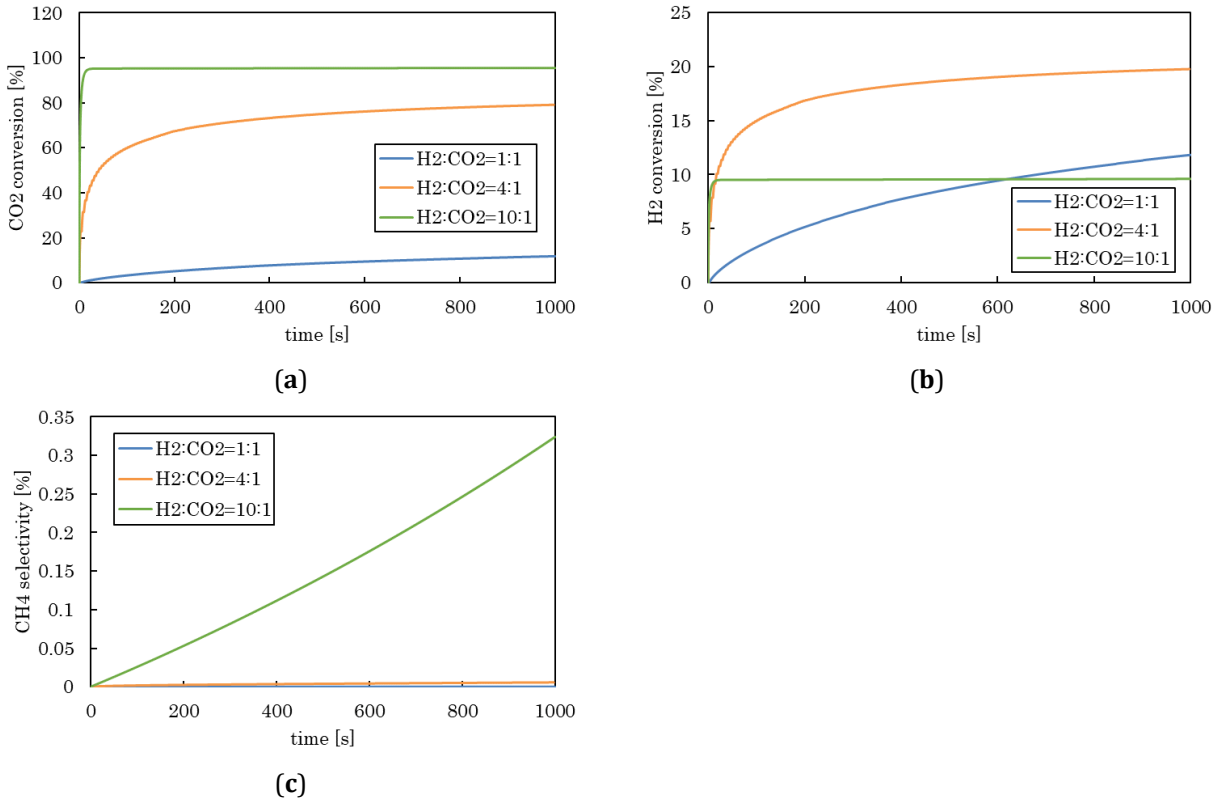

Figure 3. Effects of the initial components of reactants on the time-variations of (**a**) CO_2 conversion rate; (**b**) H_2 conversion rate; (**c**) CH_4 selectivity.

3.3. Effects of Compression Ratio

Here, we examined the effect of compression ratio, which is one of the important characteristics of the internal combustion engine. The results are shown in **Figure 4**. The initial temperature was 600 K, the initial pressure was 1 atm, and the rotational speed was 600 rpm. The compression ratio was only changed. As found in the results of the CO_2 conversion rate in **Figure 4a**, the higher the compression ratio, the higher the CO_2 conversion rate. At the compression ratio of 20, the CO_2 conversion rate reaches a steady state in about 100 s. The H_2 conversion rate is shown in **Figure 4b**. At 1000 s, the CO_2 and H_2 conversion rates are 86.8% and 21.7%, respectively. That is, the CO_2 conversion rate is very high, and the H_2 conversion rate is much lower. **Figure 4c** shows the time-variation of the CH_4 selectivity. It is noted that the higher compression ratio, the larger the CH_4 selectivity. However, the methane production rate is still very low.

Then, it is derived that the condition of the higher compression ratio can produce more methane. However, even when the compression ratio is 20, the maximum CH_4 selectivity is only 0.07%. These results indicate that Equation (2) is still the main reaction, showing that CO is formed instantly. Since the reaction rate of Equation (3) is smaller, very little methane is produced. Thus, we need to figure out a technical way to increase methane production largely.

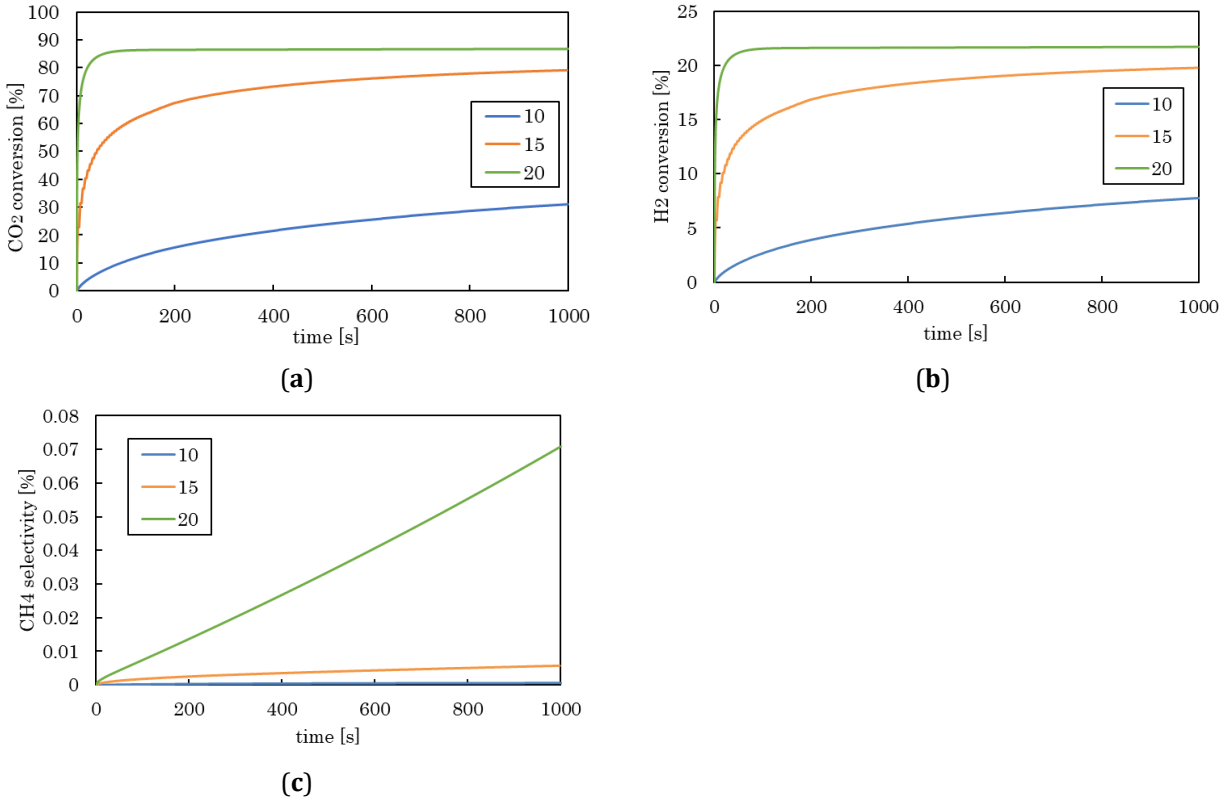

Figure 4. Effects of the compression ratio on the time-variations of (**a**) CO_2 conversion rate; (**b**) H_2 conversion rate; (**c**) CH_4 selectivity.

3.4. Effects of Rotational Speed

Finally, the effect of the rotational speed was investigated. **Figure 5** show the results when the rotational speed was varied from 300 to 900 rpm. The initial pressure was 1 atm, and the initial temperature was 600 K. The composition of the reactants was set to be H_2:CO_2 = 4:1, and the compression ratio was 15. It can be seen that the CO_2 and H_2 conversion rates slightly increase as the rotational speed is higher. When the rotational speed is 300 rpm, the CO_2 and H_2 conversion rates are 80.3% and 20.1%, respectively. Unfortunately, the maximum CH_4 selectivity is very low, which is only 0.0062% at 900 rpm.

As a result, the methane production in the MeRE could be enlarged by increasing the rotational speed. However, even when all CO_2 is consumed, the CH_4 selectivity is still low. That is, it is easy to produce CO from CO_2 in Equation (2), while the reaction which converts CO to CH_4 in Equation (3) is unlikely to take place. These findings would be useful to improve the methanation process in the MeRE, probably coupled with a plasma-assisted CO_2 methanation [29,30].

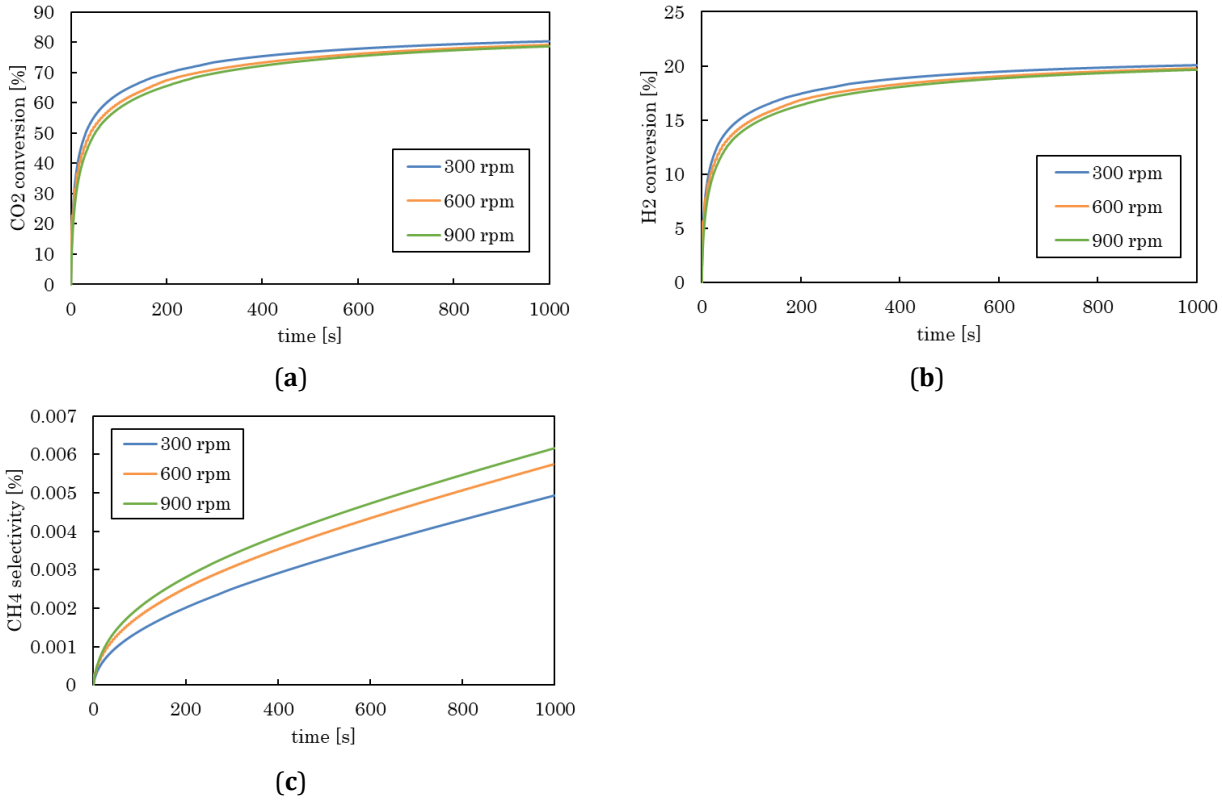

Figure 5. Effects of the rotational speed on the time-variations of (**a**) CO_2 conversion rate; (**b**) H_2 conversion rate; (**c**) CH_4 selectivity.

4. Conclusions

In this study, we have proposed the new methanation reactor, MeRE (methanation reciprocating engine). This reactor is operated by realizing the internal combustion engine. It creates a high-temperature, high-pressure field inside the reactor that is suitable for forming radicals in the reaction. To make clear the reactor characteristics based on the conversion rates, we conducted the 0-dimensional simulation using ICEN code of Chemkin-II. We focused on the initial temperature, the components of the reactants, the compression ratio, and the rotational speed. The CO_2 (or H_2) conversion rate and the CH_4 (or CO) selectivity were used to discuss favorable conditions for methane production. As the initial temperature or the compression ratio increases, CO_2 and H_2 conversion rates are larger, resulting in more CH_4 production. At the higher rotational speed, more CO_2 and H_2 are converted to form more CO and CH_4. As for the components of the reactants, it is confirmed that the composition is better to be close to the stoichiometric ratio of the Sabatier reaction. For all cases, it is found that the CO_2 conversion rate is very high, but the H_2 conversion rate is much lower. That is, even when most CO_2 is consumed, less CH_4 is produced. In other words, in case of the MeRE, it is easy to produce CO from CO_2, while the reaction which converts from CO to CH_4 is unlikely to take place.

Author Contributions

Conceptualization, K.Y.; methodology, K.Y.; software, Y.M.; validation, K.Y. and Y.M.; formal analysis, Y.M.; investigation, K.Y. and Y.M.; resources, K.Y.; data curation, Y.M.; writing—original draft preparation, K.Y. and Y.M.; writing—review and editing, K.Y.; visualization, Y.M.; supervision, K.Y.; project administration, K.Y.; funding acquisition, K.Y. All authors have read and agreed to the published version of the manuscript.

Funding

This work received no external funding.

Institutional Review Board Statement

Not applicable.

Informed Consent Statement

Not applicable.

Data Availability Statement

All data that was used for this study belongs to the Japanese Ministry of Education, Culture, Sports, Science and Technology. The dataset may be available from the corresponding author via a formal request through relevant authorities at Nagoya University in Japan.

Conflicts of Interest

The authors declare no conflict of interest.

References

1. Ghezloun, A.; Saidane, A.; Merabet, H. The COP 22 New commitments in support of the Paris Agreement. *Energy Procedia* **2017**, *119*, 10–16.
2. Musah, M.; Ahakwa, I.; Asongu, S.A.; et al. Unlocking the COP28 climate agenda in G10 economies: Do environmental taxes and environmentally - related technologies matter in the natural resource - load capacity factor connection? *Sustain. Futur.* **2024**, *8*, 100341.
3. 1.5°C - consistent benchmarks for enhancing Japan's 2030 climate target. Available from: https://climateactiontracker.org/documents/841/2021_03_CAT_1.5C-consistent_benchmarks_Japan_NDC.pdf (cited 5 March 2025).
4. Sánchez - Bastardo, N.; Schlögl, R.; Ruland, H. Methane pyrolysis for zero - emission hydrogen production: a potential bridge technology from fossil fuels to a renewable and sustainable hydrogen economy. *Ind. Eng. Chem. Res.* **2021**, *60*, 11855–11881.
5. Tada, S.; Shimizu, T.; Kameyama, H.; et al. Ni/CeO_2 catalysts with high CO_2 methanation activity and high CH4 selectivity at low temperatures. *Int J Hydrogen Energy* **2012**, *37*, 5527–5531.
6. Le, T.A.; Kim, M.S.; Lee, S.H.; et al. CO and CO_2 methanation over supported Ni catalysts. *Catal. Today* **2017**, *293–294*, 89–96.
7. Wulf, C.; Linßen, J.; Zapp, P. Review of power - to - gas projects in Europe. *Energy Procedia* **2018**, *155*, 367–378.
8. Farsi, S.; Olbrich, W.; Pfeifer, P.; Dittmeyer, R. A consecutive methanation scheme for conversion of CO_2 – A study on Ni3Fe catalyst in a short - contact time micro packed bed reactor. *Chem Eng J* **2020**, *388*, 1–11.
9. Lin, Y.; Zhang, W.; Machida, H.; Norinaga, K. CFD simulation of the Sabatier process in a shell - and - tube reactor under local thermal non - equilibrium conditions: parameter sensitivity and reaction mechanism analysis. *Int. J. Hydrogen Energy* **2022**, *47*, 15254–15269.
10. Gahleitner, G. Hydrogen from renewable electricity an international review of power - to - gas pilot plants for stationary applications. *Int. J. Hydrogen Energy* **2013**, *38* (5), 2039–2061.
11. Singh, S.; Jain, S.; Venkateswaran, P.S.; et al. Hydrogen: A sustainable fuel for future of the transport sector. *Renew. Sustain. Energy Rev.* **2015**, *51*, 623–633.
12. Er - rbib, H.; Bouallou, C. Modeling and simulation of CO methanation process for renewable electricity storage. *Energy* **2014**, *75*, 81–88.
13. Bailera, M.; Lisbona, P.; Romeo, L.M.; et al. Power to gas projects review: Lab, pilot and demo plants for storing renewable energy and CO_2. *Renew. Sustain. Energy Rev.* **2017**, *69*, 292–312.
14. de Vries, H.; Mokhov, A.V.; Levinsky, H.B. The impact of natural gas/hydrogen mixtures on the performance of end - use equipment: Interchangeability analysis for domestic appliances. *Appl. Energy* **2017**, *208*, 1007–1019.
15. Isaac, T. HyDeploy: The UK's first hydrogen blending deployment project. *Clean Energy* **2019**, *3*, 114–125.
16. Onuka, S.; Umemura, A.; Takahashi, R.; et al. Frequency control of power system with renewable power sources by HVDC interconnection line and battery considering energy balancing. *J. Power Energy Eng.* **2020**, *8*, 11–24.

17. Wang, B.; Mikhail, M.; Cavadias, S.; et al. Improvement of the activity of CO_2 methanation in a hybrid plasma - catalytic process in varying catalyst particle size or under pressure. *J. CO_2 Util.* **2021**, *46*, 2–9.
18. Takano, H.; Shinomiya, H.; Izumiya, K.; et al. CO_2 methanation of Ni catalysts supported on tetragonal ZrO_2 doped with Ca^{2+} and Ni^{2+} ions. *Int. J. Hydrogen Energy* **2015**, *40*, 8347–8355.
19. Yamamoto, K.; Sakaguchi, K. Hydrogen reactivity factor and effects of oxygen on methane conversion rate by chemical equilibrium calculation. *Int. J. Thermofluids* **2022**, *15*, 100186.
20. Yamamoto, K.; Sakaguchi, K. 1D Modeling of methanation reactor with circulation (MeRCi) for assessment of reaction characteristics. *Int. J. Thermofluids* **2023**, *20*, 100513.
21. Chemkin - II: A Fortran chemical kinetics package for the analysis of gas - phase chemical kinetics. Available from: https://www.osti.gov/biblio/5681118L (cited 5 March 2025).
22. Beuls, A.; Swalus, C.; Jacquemin, M.; et al. Methanation of CO_2: further insight into the mechanism over Rh/gamma - Al_2O_3 catalyst. *Appl. Catal. B Environ.* **2012**, *113–114*, 2–10.
23. Aldana, P.A.U.; Ocampo, F.; Kobl, K.; et al. Catalytic CO_2 valorization into CH4 on Ni - based ceria - zirconia. Reaction mechanism by operando IR spectroscopy. *Catal. Today* **2013**, *215*, 201–207.
24. Zhu, H.; Razzaq, R.; Li, C.; et al. Catalytic methanation of carbon dioxide by active oxygen material $Ce_xZr_{1-x}O_2$ supported Ni - Co bimetallic nanocatalysts. *AiChE J.* **2013**, *59*, 2567–2576.
25. Aziz, M.A.A.; Jalil, A.A.; Triwahyono, S.; et al. Highly active Ni - promoted mesostructured silica nanoparticles for CO_2 methanation. *Appl. Catal. B Environ.* **2014**, *147*, 359–368.
26. Pan, Q.; Peng, J.; Sun, T.; et al. Insight into the reaction route of CO_2 methanation: promotion effect of medium basic sites. *Catal. Commun.* **2014**, *45*, 74–78.
27. Westermann, A.; Azambre, B.; Bacariza, M.C.; et al. Insight into CO_2 methanation mechanism over NiUSY zeolites: an operando IR study. *Appl. Catal. B Environ.* **2015**, *174–175*, 120–125.
28. Kakoee, A.; Gharehghani, A. Carbon oxides methanation in equilibrium; a thermodynamic approach. *Int J Hydrogen Energy* **2020**, *45*, 29993–30008.
29. Costa, P.D.; Hasrack, G.; Bonnety, J.; et al. Ni - based catalysts for plasma - assisted CO_2 methanation. *Curr. Opin. Green Sustain. Chem.* **2021**, *32*, 100540.
30. Ullah, S.; Gao, Y.; Dou, L.; et al. Recent trends in plasma - assisted CO_2 methanation: A critical review of recent studies. *Plasma Chem. Plasma Process.* **2023**, *43*, 1335–1383.